Michigan State University

National Superconducting Cyclotron Laboratory

TRACKING FISSION-LIKE PROCESSES IN CENTRAL COLLISIONS OF $^{40}Ar + ^{232}Th$; E = 15-115 AMeV

J. YEE, E.E. GUALTIERI, D. CRAIG, S.A. HANNUSCHKE, T. LI, W.J. LLOPE, R. PAK, N.T.B. STONE, A.M. VANDER MOLEN, G.D. WESTFALL, J.S. WINFIELD, S.J. YENNELLO, R. LACEY, A. NADASEN, and E. NORBECK

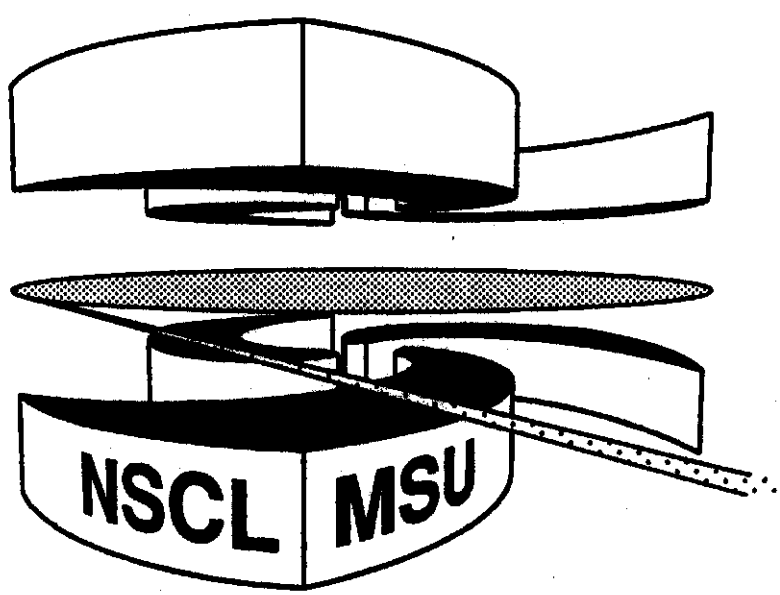

MSUCL-969 JULY 1995

Tracking Fission-like Processes in Central Collisions of $^{40}Ar + ^{232}Th$; E = 15 - 115 AMeV.

J. Yee, E. E. Gualtieri, D. Craig*, S. A. Hannuschke, T. Li, W. J. Llope†, R. Pak, N. T. B. Stone, A. M. Vander Molen, G. D. Westfall, J. S. Winfield and S. J. Yennello‡

National Superconducting Cyclotron Laboratory and Department of Physics and Astronomy, Michigan State University, East Lansing, Michigan 48824-1321, USA

Roy A. Lacey

Department of Chemistry, State University *of New York at Stony Brook Stony Brook, New York 11794-3400, USA*

A. Nadasen

Department of Natural Sciences, University of Michigan, *Dearborn, Michigan 48128, USA*

E. Norbeck

Department of Physics, University of Iowa, Iowa City, Iowa 52242, USA

(July 17, 1995)

Abstract

Fission–like fragments and coincident charged particles have been measured in a 4π geometry over a wide energy range (15 – 115 AMeV) for the reaction $^{40}Ar + ^{232}Th$. The exclusive folding angle distribution data provide direct evidence that fission–like processes following incomplete–fusion are still an appreciable exit channel for beam energies as high as 115 AMeV.

PACS number(s): 25.70.Jj, 25.70.Pq

Angular correlation studies of fission-like fragments produced via the bombardment of highly fissile targets provide important insights into nuclear reaction dynamics. Over the past several years, exhaustive studies of inclusive fragment-fragment folding angle distributions have been performed, and the results from these studies have provided a wealth of insights on linear momentum transfer and energy dissipation in heavy ion collisions [1–7].

Fragment–fragment folding angle distributions are typically characterized by two peaks; one at small folding angles ($< 180°$) and the other at large folding angles ($\approx 180°$) [4–10]. The peak at small folding angles is usually attributed to fusion-like reactions or incomplete–fusion resulting in high linear-momentum-transfer (LMT). The other peak, located at large folding angles, is linked to peripheral reactions or target–fission with small LMT. One of the prominent features of folding angle distributions is the rapid decrease of the high linear-momentum-transfer peak with increasing beam energy [4–6,9,10].

In a series of inclusive measurements, Pollacco and Conjeaud observed that the high LMT peak in the folding angle distribution for ^{40}Ar + ^{232}Th is strongly suppressed for beam energies $E_{beam} \geq 30$ AMeV, and disappears for $E_{beam} \geq 44$ AMeV [3,4]. Many speculations pertaining to the nature of central heavy ion collisions have been generated by these rather surprising results, and a few exclusive measurements have been performed with the explicit intent of addressing the fate of central Ar + Th collisions for beam energies $\geq$ 30 AMeV [10,11]. Nonetheless the detailed nature of the reaction mechanism remains unclear.

In this paper, we report results from an extensive set of ^{40}Ar + ^{232}Th measurements (E_{beam} = 15–115 AMeV) in which we have simultaneously detected light-charged particles, intermediate mass fragments (IMF: $3 \leq Z \leq 18$), and fission fragments with nearly 4π coverage. We observe direct evidence for fission–like reactions in a beam energy range where prior inclusive measurements have pointed to the possible disappearance of such processes. Earlier exclusive measurements for this system have employed setups with significantly less solid angle coverage for the simultaneous detection of fragments and light-charged particles. [10,11].

The ^{40}Ar beams [15, 25, 30, 35, 40, 45, 55, 75, and 115 AMeV] used in this experiment were provided by the K1200 cyclotron at the National Superconducting Cyclotron Laboratory (NSCL). The beam intensity was approximately 100 electrical pA and the thickness of the Th target was 1.0 mg/cm^2. Charged reaction products were detected with the fully configured MSU 4π Array [12]. The MSU 4π Array consists of a main ball of 170 phoswich detectors (arranged in 20 hexagonal and 10 pentagonal subarrays) covering angles from 23° to 157° and a forward array of 45 phoswich detectors covering angles from 7° to 18°. Thirty multiwire proportional counters (MWPCs) were installed in front of 55 Bragg curve counters (BCCs) which in turn were installed in front of the hexagonal and pentagonal phoswich sub-arrays. The MWPCs and BCCs were operated with 5 torr of isobutane gas and 125 torr of C_2F_6 gas respectively. In addition to providing Z and E signals for fragments stopped in their active volume, the BCCs provided ΔE signals for charged fragments ($Z \geq 2$) that stopped in the fast plastic scintillator of the main ball. Fission-like fragments were detected in the MWPCs with an angular resolution of $\approx 1°$. Time signals obtained from these MWPCs allowed the determination of the fragment velocities. The 4π Array provided clear Z identification for charges of Z = 1 through 18. Low energy thresholds for the main ball were 17 AMeV, 2 AMeV, and 4 AMeV for fragments of Z=1,3, and 12 respectively. The low energy threshold for the forward array was $\approx$ 17 AMeV. Data were taken with a minimum bias MWPC trigger (one or more charged fragments detected in the MWPCs).

The efficiency of MWPCs relative to BCCs rises from 25% for Z = 3 to 100% for $Z \geq 10$. Consequently, it was necessary to apply offline gates to separate the fission-like fragments from the IMFs. The fragments which stopped in the BCCs, provided two distinct groups which were identified and assigned to IMFs and fission fragments. Low energy fragments which triggered the MWPCs but left no signal in the BCCs were separated by the pulse height difference.

Folding-angle (θ_{ff}) distributions for Ar + Th are shown in Fig. 1 for E_{beam} = 15, 25, 30, 35, 45, 55, 75, and 115 AMeV. Events are selected when there are two and only two fission-like fragments (Z > 18) detected in the MWPCs, irrespective of the existence of coincident

IMFs or light charged particles. Folding angles were determined [event by event] from the directional unit vectors (**f**) of these two fission–like fragments: $\theta_{ff} = \arccos(\mathbf{f_1} \cdot \mathbf{f_2})$. The angle between the two planes defined by the beam axis and the unit vector of each fragment, ϕ_{ff}, was allowed to vary between $-90°$ and $90°$ for these distributions. The double peaked structure which is characteristic of folding angle distributions is clearly visible in Fig. 1 for beam energies $\leq$ 45 AMeV. The high and low LMT peaks are located at approximately 110° and 165°, respectively. The energy dependence of these distributions are similar to those previously reported for comparable beam energies [3,4,10]. They corroborate the previous observation that the high LMT peak essentially disappears for $E_{beam} \approx 50$ AMeV.

The top panel of Fig. 2 shows ϕ_{ff} distributions gated on the folding angle distributions shown in Fig. 1. The open circles in the figure represent the distributions gated on the low LMT peak, $\theta_{ff} > 135°$. The solid squares represent distributions gated on the high LMT peak, $85° \leq \theta_{ff} \leq 135°$. Distributions are shown for several beam energies as indicated in the figure. The widths of the gaussian curves used to fit these distributions are shown in the bottom panel of Fig. 2 with the same symbolic convention as that of the top panel. A striking feature of this figure is the beam energy dependence of the widths of the ϕ_{ff} distributions for high LMT. In contrast to the widths for the low LMT ϕ_{ff} distributions ($\approx 30°$), these widths show a monotonic increase (from 25° to 70°) with increasing beam energy. Since the target fission with low LMT is essentially a binary process, one can conclude that the high LMT reaction mechanism becomes increasingly different from a binary one as the beam energy increases. We attribute this trend to a growth in the importance of multi fragment final states [not necessarily simultaneous multifragmentation] with increasing beam energy. It appears that the suppression of the high LMT peak with increasing beam energy (cf. Fig.1) is not only associated with a decrease in the cross section for fission–like processes that follow incomplete–fusion but also with a change in reaction mechanism from an essentially binary one to non–binary one. Therefore, proper selection of multi fragment final states could lead to selective enhancement of the high LMT peak in the θ_{ff} distributions.

In Fig. 3, we compare folding angle distributions for fission-like fragments emitted in

multi fragment events. The left column of the figure (Figs. 3a - 3d) shows distributions gated on one or more IMFs at forward angles ($\theta_{lab} < 15°$). The middle column (Figs. 3e - 3h) shows distributions gated by the detection of one or more IMFs at backward angles ($\theta_{lab} > 68°$). The right column (Figs. 3i - 3l) shows distributions gated on the top 10% of the total-transverse-kinetic-energy impact parameter filter. The four rows in Fig. 3 (from top to bottom) show results for E_{beam} = 35, 45, 75, and 115 AMeV, respectively. It should be noted here that the cross sections reported in the figure are not corrected for the detection efficiency of the IMFs. In contrast to the double peaked folding angle distributions shown in Fig. 1, the distributions shown in Fig. 3 are characterized by a single peak which can be linked to either high or low LMT. The distributions gated on forward IMFs show peaks which are clearly associated with low LMT, while the distributions gated on backward IMFs or small impact parameters show the expected peaks for high LMT. As the beam energy increases, the high LMT peak can only be identified when the fission–like fragments are measured along with other particles. This fact is evident when one compares Fig. 3 to Fig. 1. It is noteworthy that the high LMT peak is well-separated from low LMT peak even at E_{beam} = 115 AMeV, which provides the direct evidence that the fission–like processes persist up to this beam energy. Moreover, the gating condition requires these events to be non–binary. We conclude that the fission–like process which follows incomplete–fusion is a well–defined exit channel for the entire beam energy range of our measurements and that it changes its characteristics from an essentially binary mechanism [at low energy] to one involving more than two fragments.

Folding angles can be translated into LMT event by event [8]. We have extracted average LMT values, $< p > /p_{beam}$, considering both target–fission as well as fusion–fission. They are estimated to be 86, 70, 62, 54, 41, 32, 23, and 16% for Figs. 1a–1h, respectively. A maximum of 151 $\pm$ 11 MeV/c per projectile nucleon is observed for $E_{beam} \approx$ 30 AMeV, which agrees with previous data [6,7]. The methods used in Fig. 3 to identify and enhance the high LMT peak make it possible for us to extract the most probable LMT as well for the entire energy range measured. A maximum of 172 $\pm$ 11 MeV/c per projectile nucleon

is obtained for $E_{beam} \approx 30$ AMeV. In spite of the difference between the average and most probable LMT values for 30 AMeV, one is still led to the conclusion that there is a limit to the amount of linear momentum that can be transferred from the projectile to the fission–like fragments. This limitation is apparently due to the fact that, with increasing beam energy, a significant fraction of the available momentum is carried away by particles other than fission–like fragments. This is the case identified in the right two columns of Fig. 3.

In order to gain insight on the evolution of the reaction mechanism, we have performed a simple two stage model calculation [13–15]. In this model the nucleons of a projectile are trapped inside the potential well of the target, and the resulting system undergoes pre–equilibrium emission of particles and then expands isentropically. Extracted percolation parameters then determine whether the system eventually experiences multifragmentation or fissions. In Fig. 4, the fission–like process cross section from the data is plotted along with the calculation. Both show that there is a substantial decrease in the cross section for fission–like reactions as the beam energy increases, but the model under-predicts the cross section in the high energy range where the non-binary fission takes over the reaction mechanism.

In conclusion, we have performed an extensive set of exclusive folding angle measurements. We see a monotonic decrease (86 % to 16 %) in momentum transfer of the projectile to the fission–like fragments with increasing beam energy. This trend is consistent with the notion that as the beam energy increases more violent collisions occur and large number of particles are ejected each carrying a fraction of the available linear momentum. Apparently the occurrence of pure binary fission seems to be less likely with increasing beam energy and a different reaction mechanism leading to multi body final states takes over. Our exclusive measurement makes it possible to observe fission–like reactions even at $E_{beam} \approx 115$ AMeV, and provide direct evidence for the persistence of these reactions albeit in non–binary form over the energy range we studied.

This work has been supported by the U.S. National Science Foundation under Grant No. PHY 92–14992.

REFERENCES

* Present Address: Department of Physics, University of Wisconsin, Madison, Wisconsin 53706, USA

† Present Address: T. W. Bonner Nuclear Laboratory, Rice University, Houston, Texas 77251–1892, USA

‡ Present Address: Cyclotron Institute, Texas A & M University, College Station, Texas 77843, USA

[1] M. Begemann-Blaich, Th. Blaich, M. M. Fowler, J. B. Wilhelmy, H. C. Britt, D. J. Fields, L. F. Hansen, R. G. Lanier, D. J. Massoletti, M. N. Namboodiri, Y. D. Chan, A. Dacal, A. Harmon, J. Pouliot, R. G. Stokstad, S. Kaufman, F. Videbaek, and Z. Fraenkel, Phys. Rev. C **45**, 677 (1992)

[2] S. Leray, G. Nebbia, C. Gregoire, G. La Rana, P. Lhenoret, C. Mazur, C. Ngô, M. Ribrag, E. Tomasi, S. Chiodelli, J. L. Charvet, and C. Lebrun, Nucl. Phys. **A425**, 345 (1984)

[3] E. C. Pollacco, M. Conjeaud, S. Harar, C. Volant, Y. Cassagnou, R. Dayras, R. Legrain, M. S. Nguyen, H. Oeschler, and F. Saint-Laurent, Phys. Lett. **146B**, 29 (1984)

[4] M. Conjeaud, S. Harar, M. Mostefai, E. C. Pollacco, C. Volant, Y. Cassagnou, R. Dayras, R. Legrain, H. Oeschler, and F. Saint-Laurent, Phys. Lett. **159B**, 244 (1985)

[5] D. Jacquet, E. Duek, J. M. Alexander, B. Borderie, J. Galin, D. Gardes, D. Guerreau, M. Lefort, F. Monnet, M. F. Rivet, and X. Tarrago, Phys. Rev. Lett. **53**, 2226 (1984)

[6] V. E. Viola, Nucl. Phys. **A502**, 531c (1989)

[7] M. B. Tsang, D. R. Klesch, C. B. Chitwood, D. J. Fields, C. K. Gelbke, W. G. Lynch, H. Utsunomiya, K. Kwiatkowski, V. E. Viola Jr., and M. Fatyga, Phys. Lett. **134B**, 169, (1984)

[8] H. K. W. Leegte, A. L. Boonstra, J. D. Hinnefeld, E. E. Koldenhof, R. H. Siemssen, K. Siwek-Wilczyńska, Z. Sosin, J. Wilczyński, and H. W. Wilschut, Phys. Rev. C **46**, 991 (1992)

[9] M. Fatyga, K. Kwiatkowski, V. E. Viola, C. B. Chitwood, D. J. Fields, C. K. Gelbke, W. G. Lynch, J. Pochodzalla, M. B. Tsang, and M. Blann, Phys. Rev. Lett. **55**, 1376 (1985)

[10] E. Schwinn, U. Jahnke, J. L. Charvet, B. Cramer, H. Doubre, J. Fréhaut, J. Galin, B. Gatty, D. Guerreau, G. Ingold, D. Jacquet, D. X. Jiang, B. Lott, M. Morjean, C. Magnago, Y. Patin, J. Pouthas, E. Piasecki, and A. Sokolow, Nucl. Phys. **A568**, 169 (1994).

[11] D. X. Jiang, H. Doubre, J. Galin, D. Guerreau, E. Piasecki, J. Pouthas, A. Sokolov, B. Cramer, G. Ingold, U. Jahnke, E. Schwinn, J. L. Charvet, J. Frehaut, B. Lott, C. Magnago, M. Morjean, Y. Patin, Y. Pranal, J. L. Uzureau, B. Gatty, and D. Jacquet, Nucl. Phys. **A503**, 560 (1989)

[12] G. D. Westfall, J. E. Yurkon, J. Van Der Plicht, Z. M. Koenig, B. V. Jacak, R. Fox, G. M. Crawley, M. R. Maier, and B. E. Hasselquist, Nucl. Inst. and Meth. **A238**, 347 (1985)

[13] G. D. Harp, and J. M. Miller, Phys. Rev. C **3**, 1847 (1971)

[14] J. Desbois, R. Boisgard, C. Ngô, and J. Nemeth, Z. Phys. **A328**, 101 (1987)

[15] C. Cerruti, R. Boisgard, C. Ngô and J. Desbois, Nucl. Phys. **A492**, 322 (1989)

FIGURES

Fig. 1: Inclusive fission fragment folding angle distributions for Ar + Th reactions from 15 to 115 AMeV.

Fig. 2: [Top panel] Fission fragment azimuthal distributions for Ar + Th reaction from 15 to 115 AMeV gated on high LMT (solid squares) and low LMT (open circles). Even though it decreases substantially with beam energy, the high LMT distribution maintains its gaussian shape. [Bottom panel] Widths of gaussian distributions used to fit the data in top panel vs. beam energy. The symbols follow the same convention.

Straight lines are to guide the eye.

Fig. 3: Fission fragment folding angle distributions for Ar + Th reactions gated on IMFs at forward angles (left column), IMFs at large angles (center column), and central collision impact parameter obtained by the total transverse kinetic energy. Solid lines are gaussian fits to guide the eye.

Fig. 4: Comparison of the extracted fission–like process cross sections for Ar + Th data (solid circles) with the predictions of the model (open circles). Lines are drawn to guide the eye.

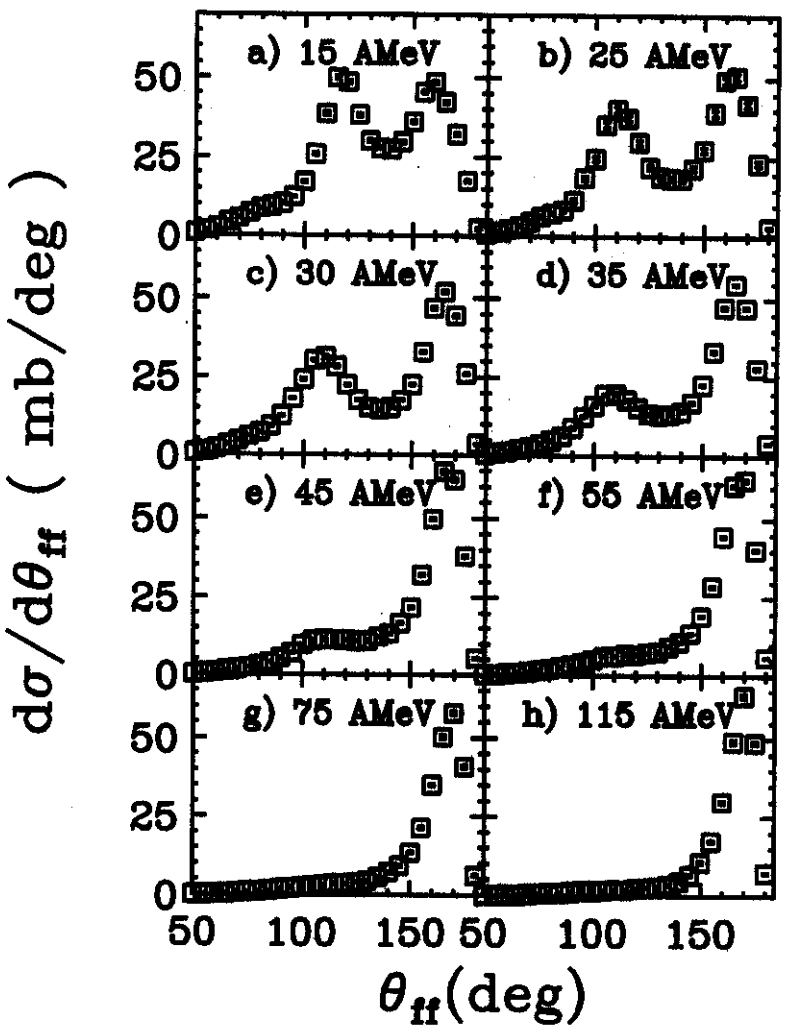
a) 15 AMeV
b) 25 AMeV
c) 30 AMeV
d) 35 AMeV
e) 45 AMeV
f) 55 AMeV
g) 75 AMeV
h) 115 AMeV
50
25
0
50 100 150 50 100 150
dσ/dθff (mb/deg)
θff(deg)

Fig. 1.

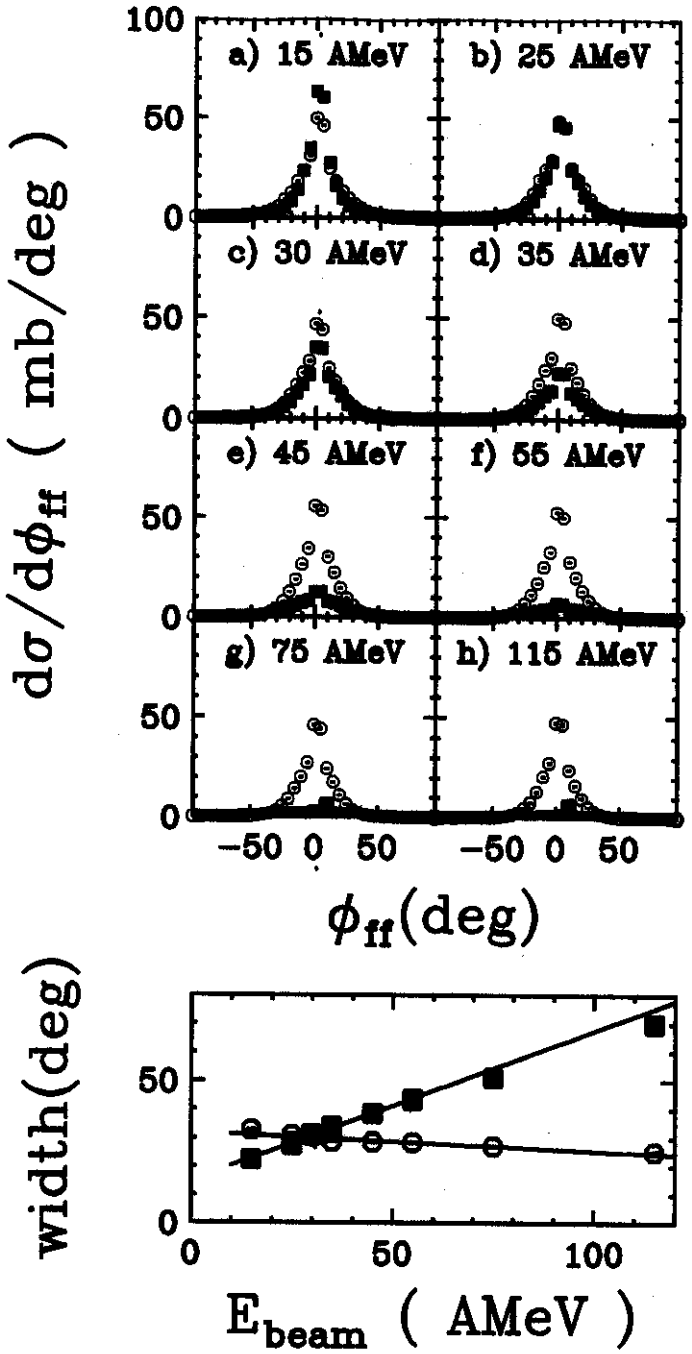
a) 15 AMeV
b) 25 AMeV
c) 30 AMeV
d) 35 AMeV
e) 45 AMeV
f) 55 AMeV
g) 75 AMeV
h) 115 AMeV
100
50
0
−50 0 50
dσ/dφff (mb/deg)
φff(deg)
width(deg)
Ebeam (AMeV)

Fig. 2.

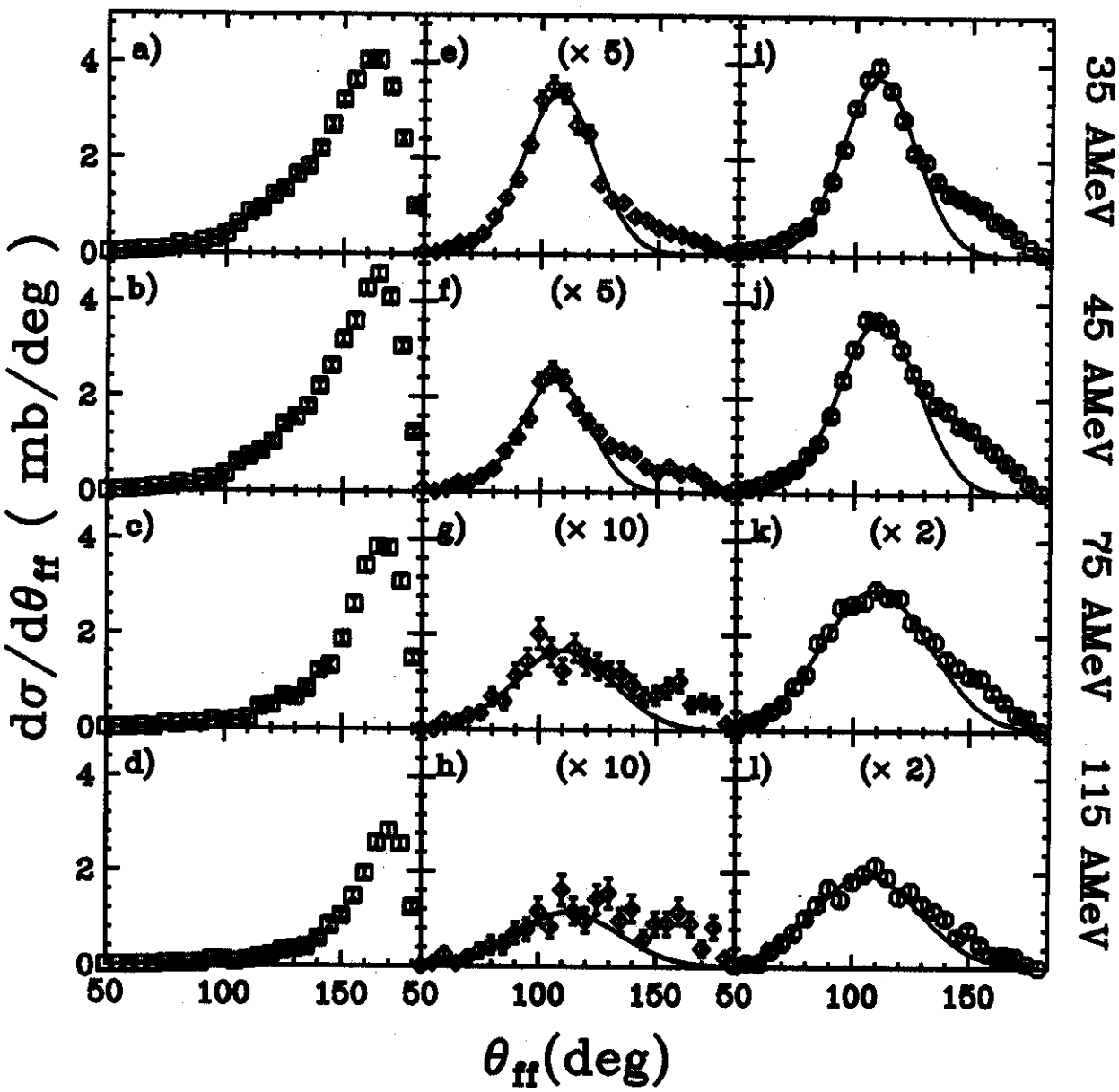
a)
b)
c)
d)
e)
(× 5)
f)
(× 5)
g)
(× 10)
h)
(× 10)
i)
j)
k)
(× 2)
l)
(× 2)
35 AMeV
45 AMeV
75 AMeV
115 AMeV
dσ/dθff (mb/deg)
θff(deg)
0
2
4
50
100
150

Fig. 3.

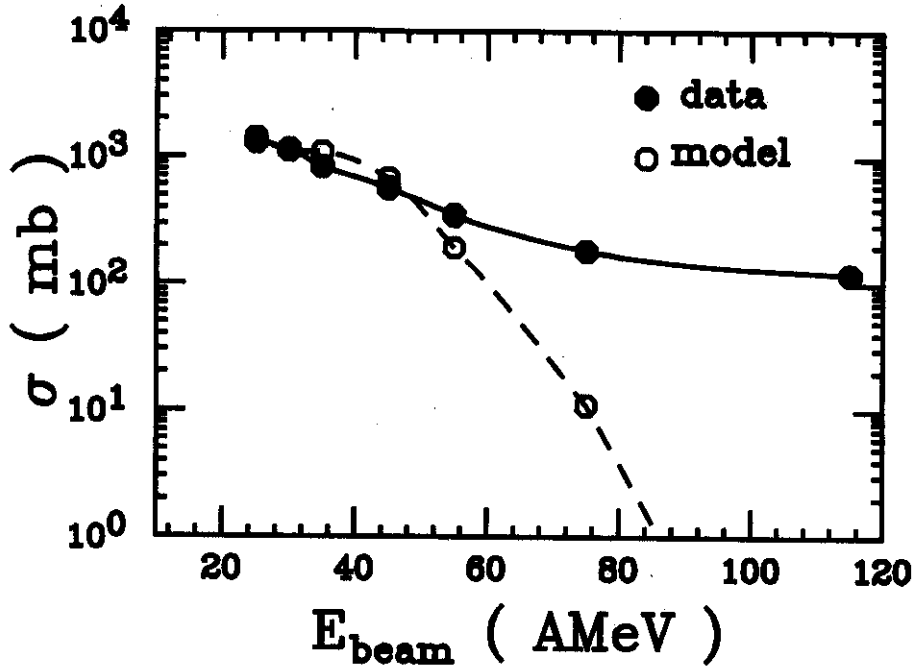
data
model
σ (mb)
10^4
10^3
10^2
10^1
10^0
20
40
60
80
100
120
E_{beam} (AMeV)

Fig. 4.